Progress In Electromagnetics Research C, Vol. 109, 13–26, 2021

A Feed-Forward Control Strategy for Compensating Rotor Vibration of Six-Pole Radial Hybrid Magnetic Bearing with Fuzzy Adaptive Filter

Huangqiu Zhu and Mingjie Tang*

Abstract—In order to solve the problem that the unbalance vibration caused by rotor mass eccentricity of the six-pole radial hybrid magnetic bearing (HMB) seriously affects stability and security of the system, a feed-forward compensation control strategy for rotor unbalance vibration based on fuzzy least-mean-square (LMS) algorithm is proposed. Firstly, the structure, operation principle, and mathematical model of the six-pole radial HMB are introduced, and the cause of rotor vibration is analyzed and the dynamic equation of rotor deduced. Secondly, an LMS self-adapting filter is improved by using a fuzzy inference system, and the step size of the LMS algorithm is combined with the fuzzy control theory. By using the Takagi-Sugeno (TS) fuzzy inference machine system to adjust the step size of the algorithm, the filter output can approach the unbalance vibration signal smoothly and quickly, and realize the vibration compensation of the rotor. Finally, the simulations and experiments are carried out to verify that the proposed method can not only effectively suppress the unbalance vibration of the six-pole radial HMB rotor in real time but also have good compensation accuracy. The results show that the vibration compensation effect of fuzzy LMS algorithm is better than that of fixed step size filtering algorithm.

1. INTRODUCTION

Magnetic bearing is a kind of supporting device which uses magnetic field force to suspend the rotor stably in the equilibrium position and achieves no mechanical contact between the rotor and the stator. So the magnetic bearing has the advantages of no friction, no wear, no lubrication, high speed, and high precision, and can be widely used in life science, energy transportation, industrial manufacturing, aerospace, and other fields [1–3].

The bias magnetic flux of the hybrid magnetic bearing (HMB) is generated by a permanent magnet, which can reduce the system power consumption and control circuit volume, save costs, and have the advantages of high efficiency and compact structure [4–6]. Six-pole radial HMB adopts a double-slice structure, which improves the nonlinearity and coupling caused by structural asymmetry, and has great research significance. However, practice shows that when the rotor rotates at a high speed, due to the defects of the mechanical processing of the motor rotor, the rotor cannot avoid eccentricity, and a unique periodic vibration problem occurs, which seriously affects the rotor rotation accuracy and system stability. So, the study of compensation for unbalance vibration of magnetic bearing rotor is a very important subject [7, 8].

The vibration compensation control of rotor has been studied extensively. Magnetic bearings generally have two control modes for rotor unbalance vibration. One is automatic balance, and the other is unbalance compensation. The unbalance compensation method extracts the vibration signal with the same frequency as the rotation speed to generate a certain control force to balance the unbalance

Received 10 December 2020, Accepted 11 January 2021, Scheduled 21 January 2021
* Corresponding author: Mingjie Tang (DYtangmingjie@163.com).
The authors are with the School of Electrical and Information Engineering, Jiangsu University, Zhenjiang 212013, China.

force and make the rotor rotate around its geometric axis [9, 10]. In order to suppress synchronous vibration of the magnetic bearing rotor with gyroscopic effect and coupling, a novel cross-feedback notch filter is proposed in [11]. The experimental results show that this method has remarkable effect on the suppression of synchronous vibration and the maintenance of stability. Aiming at the output regulator problem of input delay system, an unbalance compensation method for active magnetic bearing with input delay is proposed in [12]. An unbalance compensator based on the real-time variable step polygon iterative extraction algorithm is proposed in [13], which can effectively suppress the unbalance vibration of the rotor of active magnetic bearing in steady state and variable speed operation. Automatic balance method eliminates the unbalance vibration component in the displacement signal by filtering or offsetting to make the rotor rotate around its inertial axis [14]. In terms of automatic balancing, an adaptive compensation algorithm to compensate the displacement stiffness by generating the target coil current is designed in [15]. This method can automatically compensate the change of power amplifier and induction electromotive force to realize the suppression of vibration force and vibration torque. In order to suppress the multi-frequency vibration in the rotor system of AMB high-speed motor, a method to control the multi-frequency vibration of rotor system by current compensation is proposed in [16]. The variable step triangular iterative search algorithm is used to accelerate the recognition of multi-frequency current coefficient and improve the compensation effect. Due to the advantages of simple calculation, simple structure, good robustness, and tracking performance, the least-mean-square (LMS) algorithm is also widely used in the study of vibration compensation for magnetic bearing rotors [17]. However, there are some problems in the process of using LMS algorithm for rotor vibration compensation control. The smaller the algorithm step size is, the smaller the error is when reaching steady state, but the slower the tracking speed of the system is. The larger the step size of the algorithm is, the faster the tracking speed of the system is, but the greater the error is when it reaches the steady state, which leads to insufficient compensation accuracy. Therefore, when the fixed step LMS algorithm is used, there is a difficult contradiction between the tracking speed and steady-state error of the system, which cannot meet their requirements at the same time.

A fuzzy adaptive filter is used as a feed-forward compensation controller in this paper, and LMS algorithm is used to provide an unbalance vibration compensation signal for the magnetic bearing rotor system. Aiming at the problem that tracking speed and steady-state error cannot be taken into account simultaneously in the process of rotor vibration compensation control using fixed step size LMS algorithm, the concept of fuzzy control is introduced in this paper. The TS fuzzy inference machine is designed to control the size of the LMS algorithm step size, so that the step size factor can be adjusted according to the actual feedback error signal. As a result, the output signal of the filter can be quickly approximated to the expected compensation signal, and the steady-state error of rotor is not too large, which improves the effect of unbalance vibration compensation for the HMB rotor system.

2. MODELING OF SIX-POLE RADIAL HMB ROTOR

2.1. Structure Principle and Mathematical Model

The six-pole radial HMB adopts a two-piece structure. As Fig. 1 shows, the permanent magnet is annular and magnetized along the axial direction. In Fig. 1, 1 is the permanent magnet, 2 the stator, 3 the control coil, 4 the rotor, 5 the control flux, and 6 the bias flux. The structures of the left and right stator sheets are the same, consisting of a circular stator yoke and six magnetic poles uniformly distributed along the circumference, which are symmetrically placed on the left and right sides.

The magnetic flux of the six-pole radial HMB consists of two parts: bias flux and control flux. The bias flux flows out from the N pole of the permanent magnet and enters the stator yoke, magnetic pole, air gap, rotor, and returns to the S pole of the permanent magnet. The bias flux is oriented towards the center of the circle in the air gap on the left and deviates from the center in the right air gap. When the incoming current in the control coil of a certain phase is positive, the control flux pointing to the center of the circle is generated in one side of the magnetic pole and air gap, and the control flux away from the center of the circle is generated in the other side of the magnetic pole and air gap. At this time, the control flux and bias flux are in the same direction and superimposed on each other, resulting in the suspension force along the direction of the phase magnetic pole. Conversely, when the incoming current is negative, the suspension force in the direction of the magnetic pole decreases.

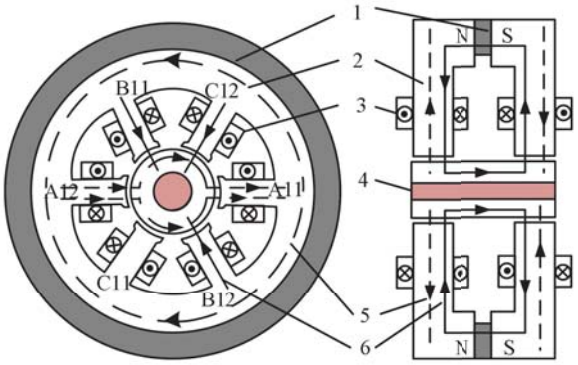

Figure 1. Structure of six-pole radial HMB.

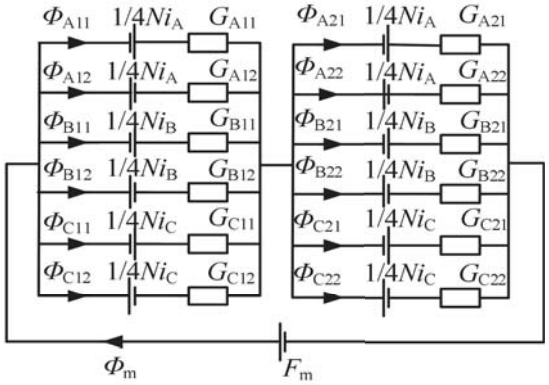

Figure 2. Equivalent magnetic circuit.

As Fig. 2 shows, Φ_m is the total bias flux. N is the total number of turns per phase coil. F_m is the magnetomotive force of the permanent magnet. Φ_{j11}, Φ_{j12}, Φ_{j21}, Φ_{j22} (j = A, B, C) are the per-pole fluxes. i_A, i_B, i_C are the inverter currents. If the radial displacement ofs rotor are x, y, then

$$\begin{cases} \Phi_{\mathrm{A11}} = \Phi_{\mathrm{A21}} = \dfrac{\mu_0 S_{\mathrm{r}}(2F_{\mathrm{m}} + Ni_{\mathrm{A}})}{4(\delta_{\mathrm{r}} - x)} \\ \Phi_{\mathrm{A12}} = \Phi_{\mathrm{A22}} = \dfrac{\mu_0 S_{\mathrm{r}}(2F_{\mathrm{m}} - Ni_{\mathrm{A}})}{4(\delta_{\mathrm{r}} + x)} \\ \Phi_{\mathrm{B11}} = \Phi_{\mathrm{B21}} = \dfrac{\mu_0 S_{\mathrm{r}}(2F_{\mathrm{m}} + Ni_{\mathrm{B}})}{4(\delta_{\mathrm{r}} + 0.5x - \sqrt{3}y/2)} \\ \Phi_{\mathrm{B12}} = \Phi_{\mathrm{B22}} = \dfrac{\mu_0 S_{\mathrm{r}}(2F_{\mathrm{m}} - Ni_{\mathrm{B}})}{4(\delta_{\mathrm{r}} - 0.5x + \sqrt{3}y/2)} \\ \Phi_{\mathrm{C11}} = \Phi_{\mathrm{C21}} = \dfrac{\mu_0 S_{\mathrm{r}}(2F_{\mathrm{m}} + Ni_{\mathrm{C}})}{4(\delta_{\mathrm{r}} + 0.5x + \sqrt{3}y/2)} \\ \Phi_{\mathrm{C12}} = \Phi_{\mathrm{C22}} = \dfrac{\mu_0 S_{\mathrm{r}}(2F_{\mathrm{m}} - Ni_{\mathrm{C}})}{4(\delta_{\mathrm{r}} - 0.5x - \sqrt{3}y/2)} \end{cases} \tag{1}$$

where δ_r is the radial air gap length, S_r the area of the pole, and μ_0 the vacuum permeability, then

$$F_j = \left(\frac{\Phi_{j11}^2}{2\mu_0 S_{\mathrm{r}}} - \frac{\Phi_{j12}^2}{2\mu_0 S_{\mathrm{r}}} \right) \times 2 \, (j = \mathrm{A}, \mathrm{B}, \mathrm{C}) \tag{2}$$

The suspension force formula is extended near the equilibrium position by Taylor's formula. On the basis of ignoring the dimensionless above two ranks, the formula of suspension force can be obtained as follows:

$$\begin{cases} F_{\mathrm{A}} = k_{xy} \cdot x + k_{i\mathrm{r}} \cdot i_{\mathrm{A}} \\ F_{\mathrm{B}} = -\dfrac{1}{2} k_{xy} \cdot x + \dfrac{\sqrt{3}}{2} k_{xy} \cdot y + k_{i\mathrm{r}} \cdot i_{\mathrm{B}} \\ F_{\mathrm{C}} = -\dfrac{1}{2} k_{xy} \cdot x - \dfrac{\sqrt{3}}{2} k_{xy} \cdot y + k_{i\mathrm{r}} \cdot i_{\mathrm{C}} \end{cases} \tag{3}$$

where $k_{xy} = \frac{2\mu_0 S_{\mathrm{r}} F_{\mathrm{m}}^2}{\delta_{\mathrm{r}}^3}$ and $k_{i\mathrm{r}} = \frac{\mu_0 S_{\mathrm{r}} F_{\mathrm{m}} N}{\delta_{\mathrm{r}}^2}$ are radial force-displacement coefficient and radial force-current coefficient, respectively.

The suspension force model is obtained by Clark transformation as follows:

$$\begin{bmatrix} F_x \\ F_y \end{bmatrix} = \frac{3}{2} k_{xy} \cdot \begin{bmatrix} 1 & 0 \\ 0 & 1 \end{bmatrix} \begin{bmatrix} x \\ y \end{bmatrix} + k_{i\mathrm{r}} \cdot \begin{bmatrix} 1 & -\dfrac{1}{2} & -\dfrac{1}{2} \\ 0 & -\dfrac{\sqrt{3}}{2} & \dfrac{\sqrt{3}}{2} \end{bmatrix} \begin{bmatrix} i_{\mathrm{A}} \\ i_{\mathrm{B}} \\ i_{\mathrm{C}} \end{bmatrix} \tag{4}$$

2.2. Mechanism Analysis of Causes of Rotor Vibration

An unbalance vibration occurs when an object rotates at high speed. Unbalance vibration can be divided into two types: static imbalance and dynamic imbalance.

The static imbalance is mainly due to mass eccentricity, as shown in Fig. 3. M is the axis of the rotor, which is the geometric center of the rotor. D is the centroid of the rotor, and λ is the distance from the centroid D to the axis M. When the rotor rotates at a certain speed, a centrifugal force is generated due to the rotor eccentricity. This centrifugal force will lead to the periodic vibration of the rotor and even transfer to the seat, resulting in the instability of the magnetic bearing system.

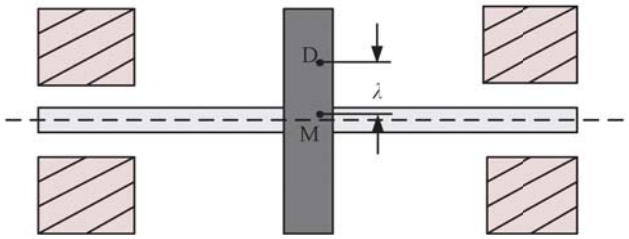

Figure 3. Static imbalance.

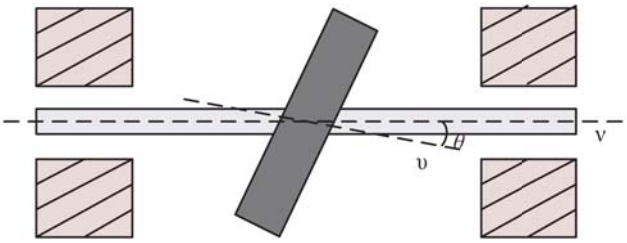

Figure 4. Dynamic imbalance.

The dynamic imbalance is mainly due to the inertia axis of the rotor ν which is not in a straight line with its rotating axis υ, forming a certain angle θ. Vibration occurs when the rotor rotates at high speed, as shown in Fig. 4.

Whether static imbalance or dynamic imbalance, it will cause the rotor to vibrate at high speed. For the six-pole HMB rotor system studied in this paper, because the stiffness of the rotor is very strong, and the two ends of the rotor are equipped with a bearing protection device, the unbalance vibration of the rotor is mainly caused by static imbalance. The unbalance vibration compensation control strategy studied in this paper is aimed at the vibration caused by static imbalance.

2.3. Kinetic Equation for Rotor of Magnetic Bearing

As Fig. 5 shows, the rotor produces centrifugal force due to mass eccentricity, resulting in unbalance vibration, and the rotor geometric center does not coincide with the center of mass. xy is the stationary coordinate system, dp the rotating speed synchronous rotation coordinate system, $M(x_\alpha, y_\alpha)$ the rotor

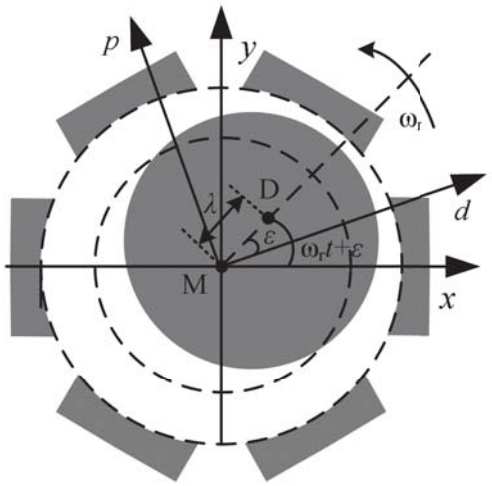

Figure 5. Rotor mass eccentricity.

geometric center, and $D(x_\beta, y_\beta)$ the rotor centroid. The geometric coordinate relations of $M(x_\alpha, y_\alpha)$ and $D(x_\beta, y_\beta)$ can be expressed as:

$$\begin{cases} x_\beta = x_\alpha + \lambda \cos(\omega_{\mathrm{r}} t + \varepsilon) \\ y_\beta = y_\alpha + \lambda \sin(\omega_{\mathrm{r}} t + \varepsilon) \end{cases} \tag{5}$$

where λ is the distance of mass eccentricity. ω_r is the rotor mechanical angular velocity. ε is the initial mass eccentricity directional angle.

As the rotor rotates at angular velocity ω_r, the unbalance vibration centrifugal force due to mass eccentricity can be expressed as:

$$F_{\mathrm{M}} = m\lambda\omega_{\mathrm{r}}^2 \tag{6}$$

where m is the quality of the rotor.

It can be seen from Eq. (6) that the magnitude of the centrifugal force generated is proportional to the square of the rotor speed, that is, the higher the rotational speed is, the more violent the unbalance vibration of the rotor will be. When the rotor system is running at high speed, the accuracy of the rotor and the stability of the system will be seriously affected.

Because the direction of centrifugal force produced during rotation is always consistent with the direction of rotor mass eccentricity, the direction of centrifugal force will also change periodically with the rotation of rotor. In a stationary coordinate system, the dynamic form of centrifugal force can be expressed as:

$$F_{\mathrm{M}} = m\lambda\omega_{\mathrm{r}}^2 e^{j(\omega_{\mathrm{r}} t + \varepsilon)} \tag{7}$$

Their components on the x- and y-axes can be expressed as:

$$\begin{cases} F_{\mathrm{M}x} = m\lambda\omega_{\mathrm{r}}^2 \cos(\omega_{\mathrm{r}} t + \varepsilon) \\ F_{\mathrm{M}y} = m\lambda\omega_{\mathrm{r}}^2 \sin(\omega_{\mathrm{r}} t + \varepsilon) \end{cases} \tag{8}$$

If the gyroscopic effect is not taken into account, according to Newton's law, the vibration equation of rotor radial displacement caused by rotor mass eccentricity can be expressed as:

$$\begin{cases} m\frac{\mathrm{d}^2 x_\alpha}{\mathrm{d}^2 t} + c_x \dfrac{\mathrm{d}x_\alpha}{\mathrm{d}t} + k_x x_\alpha = m\lambda\omega_{\mathrm{r}}^2 \cos(\omega_{\mathrm{r}} t + \varepsilon) \\ m\dfrac{\mathrm{d}^2 y_\alpha}{\mathrm{d}^2 t} + c_y \dfrac{\mathrm{d}y_\alpha}{\mathrm{d}t} + k_y y_\alpha = m\lambda\omega_{\mathrm{r}}^2 \sin(\omega_{\mathrm{r}} t + \varepsilon) \end{cases} \tag{9}$$

where c_x, c_y, k_x, k_y represent the damping and stiffness of the rotor system in the horizontal and vertical directions, respectively, then

$$\begin{cases} x_\alpha = \mathrm{A} \cos(\omega_{\mathrm{r}} t + \varepsilon - \eta) \\ y_\alpha = \mathrm{B} \sin(\omega_{\mathrm{r}} t + \varepsilon - \delta) \end{cases} \tag{10}$$

where A and B are the displacement amplitudes along the x, y axes caused by the rotor eccentricity, respectively. η and δ are the angles related to the rotor speed, rotor mass, coupling parameters, and stiffness coefficient.

It can be seen from Eq. (10) that under the influence of centrifugal force produced by the mass eccentricity of the rotor, the radial displacement of the rotor has periodic fluctuation, that is, the unbalance vibration of the rotor occurs.

3. UNBALANCE VIBRATION COMPENSATION BASED ON FUZZY ADAPTIVE FILTER

LMS adaptive filtering algorithm, as a gradient algorithm, can accurately track the frequency and phase, constantly approach the target, and keep the filter stable when the external disturbance changes. As shown in Fig. 6.

Set the basic input as:

$$\mathrm{d}(k) = s(k) + A_0 \cos(\omega_0 k + \phi_0) \tag{11}$$

where $s(k)$ is the required signal, A_0 the amplitude of sinusoidal interference, ω_0 the normalized angular frequency, and φ_0 the phase.

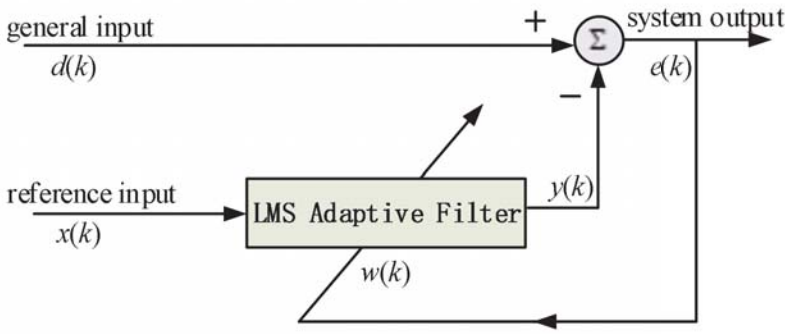

Figure 6. Schematic illustration of LMS adaptive filter.

Set the reference input as:

$$x\left(k\right)=\mathrm{A}\cos\left(\omega_0 k+\phi\right) \tag{12}$$

where the amplitude A and phase φ are different from the physical quantities of basic input, but the angular frequency ω_0 is the same.

If the LMS algorithm in the form of real numbers is used, the update of weights is based on the following equation:

$$y\left(k\right)=\sum_{i=0}^{M-1}w_i\left(k\right)x\left(k-i\right) \tag{13}$$

$$e\left(k\right)=d\left(k\right)-y\left(k\right) \tag{14}$$

$$w_i\left(k+1\right)=w_i\left(k\right)+\mu x\left(k-i\right)e\left(k\right)\quad i=0,1,\ldots,M-1 \tag{15}$$

where M is the length of the transverse filter, and the constant μ is the step size factor. The sine excitation input $x(k)$ and the weight updating equation of the LMS algorithm are combined into a single open loop system. The results are as follows:

$$\begin{aligned}x\left(k-i\right)&=A\cos\left[\omega_0\left(k-i\right)+\phi\right]\\&=\frac{A}{2}\left[e^{j(\omega_0 k+\phi_i)}+e^{-j(\omega_0 k+\phi_i)}\right]\end{aligned} \tag{16}$$

where

$$\phi_i=\phi-\omega_0 i \tag{17}$$

The input $x(k-i)$ is multiplied by the estimated error $e(k)$, and their product is obtained by z transformation. The results are as follows:

$$z[x\left(k-i\right)e\left(k\right)]=\frac{A}{2}e^{j\phi_i}E\left(ze^{-j\omega_0}\right)+\frac{A}{2}e^{-j\phi_i}E\left(ze^{j\omega_0}\right) \tag{18}$$

After z transformation, Equation (15) is expressed as:

$$zW_i\left(z\right)=W_i\left(z\right)+\mu z[x\left(k-i\right)e\left(k\right)] \tag{19}$$

By substituting Equation (18) into Equation (19), the result can be expressed as:

$$W_i\left(z\right)=\frac{\mu A}{2}\frac{1}{z-1}\left[e^{j\phi_i}E\left(ze^{-j\omega_0}\right)+e^{-j\phi_i}E\left(ze^{j\omega_0}\right)\right] \tag{20}$$

By substituting Equation (16) into Equation (13) and after z transformation, the result can be expressed as:

$$Y\left(z\right)=\frac{A}{2}\sum_{i=0}^{M-1}\left[e^{j\phi_i}W_iE\left(ze^{-j\omega_0}\right)+e^{-j\phi_i}W_iE\left(ze^{j\omega_0}\right)\right] \tag{21}$$

By substituting Equation (20) into Equation (21), the result can be expressed as:

$$Y(z) \approx \frac{\mu M A^2}{4} E(z) \left(\frac{1}{z e^{-j\omega_0} - 1} + \frac{1}{z e^{j\omega_0} - 1} \right) \tag{22}$$

Hence, the open loop transfer function $G(z)$ is

$$G(z) = \frac{Y(z)}{E(z)} \approx \frac{\mu M A^2}{4} \left(\frac{1}{z e^{-j\omega_0} - 1} + \frac{1}{z e^{j\omega_0} - 1} \right) \tag{23}$$

$$\approx \frac{\mu M A^2}{4} E(z) \left(\frac{z \cos \omega_0 - 1}{z^2 - 2z \cos \omega_0 + 1} \right) \tag{24}$$

Because

$$H(z) = \frac{1}{1 + G(z)}, \tag{25}$$

$$H(z) \approx \frac{z^2 - 2z \cos \omega_0 + 1}{z^2 - 2\left(1 - \mu M A^2/4\right) z \cos \omega_0 + \left(1 - \mu M A^2/2\right)} \tag{26}$$

The zero points in the formula are $z_0 = e^{\pm 2j\omega_0}$. When the desired signal frequency ω is equal to the input signal frequency ω_0, $H(z)$ is 0, and the filter realizes fixed frequency point filtering.

The principle of vibration compensation by adaptive filter is to input the sine cosine signal with the same frequency as the speed at the reference input, and the sine cosine signal is always the same frequency as the speed. The adaptive LMS algorithm is used to adjust the weight coefficient of the reference input signal to obtain the estimated compensation signal which can compensate the rotor vibration displacement. Finally, by subtracting the compensation signal from the main signal, the unbalanced vibration component in the displacement signal is eliminated. Because the error signal obtained by subtraction is input into the LMS algorithm to update the weight coefficient, after repeated iterations, the effect of vibration compensation is finally achieved, as shown in Fig. 7.

It should be note that the step size of the LMS algorithm is a very important parameter. Therefore, when selecting the LMS algorithm as an adaptive filtering algorithm, we need to carefully consider the

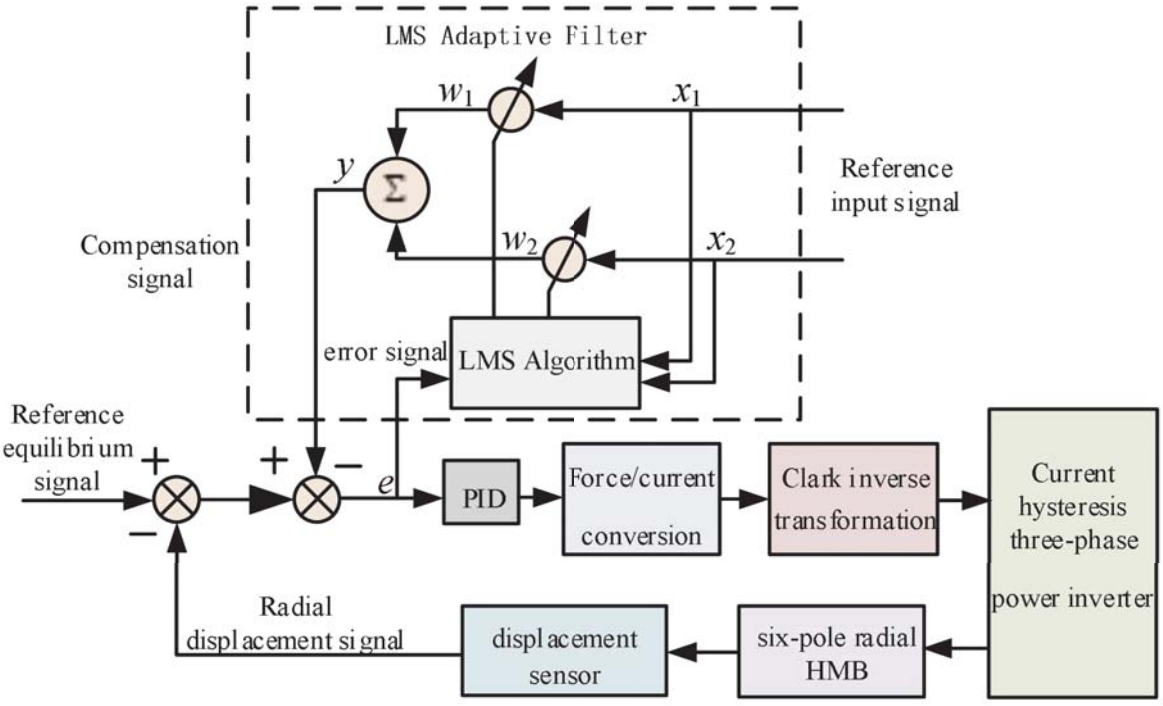

Figure 7. Schematic diagram of vibration compensation by LMS adaptive filter.

value of the step size. In order to overcome the contradiction between the tracking speed of the filter and the steady-state error of the rotor system when the step size of the algorithm is fixed, the fuzzy step size LMS algorithm combines fuzzy control with adaptive approach and uses the fuzzy inference system to determine the step size of the filtering algorithm. The fuzzy inference system in this paper uses a first-order TS fuzzy inference machine.

Since both the error e and error variation de are closely related to the step size μ, e and de are selected as the system input, and the output of the system is μ. e is divided into three fuzzy sets: small (S), medium (M), large (L). de is also divided into three fuzzy sets: negative (N), zero (Z), positive (P). The triangular membership function is chosen to achieve blurring, as shown in Fig. 8. The output μ of the system is also divided into three levels: small (S), medium (M), large (L).

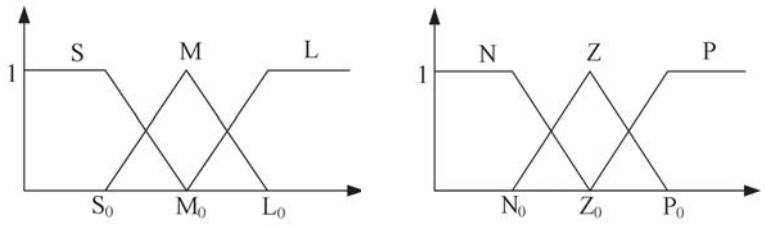

Figure 8. Membership function.

The fuzzy inference system uses a first-order TS fuzzy inference machine, which makes R_i represent the i-th rule of the fuzzy system. The first-order fuzzy conditional statement is

$$R^i\text{: IF } x_1 \text{ is } A_1^i \text{ and } \ldots \text{ and } x_n \text{ is } A_n^i \text{ then } y^i = \mathrm{a}_0^i + \mathrm{a}_1^i x_1 + \ldots + \mathrm{a}_n^i x_n$$

where x_n represents the n-th input variable in the i-th rule, $n = 1, 2, 3 \ldots k$. A_n^i represents the fuzzy set corresponding to x_n in the i-th rule, and y^i represents the output of the i-th rule. a_n^i represents the parameter corresponding to x_n of the i-th rule. It can be seen that the output of the TS fuzzy inference machine directly contains the linear combination of the input signals, which is more suitable for the adjustment of fuzzy control rules.

The input of the fuzzy control system in this paper is e and de, and the output is μ. As Fig. 9 shows, by blurring the variation of the error signal de and the error signal e, the step size of the LMS algorithm μ is obtained according to the output function $\mu^j = a_0^j + a_1^j e + a_2^j de$. TS fuzzy control structure diagram is shown in Fig. 10. The first column inputs the actual signal; the second column is to blur; the third and fourth columns are fuzzy reasoning; and the fifth column gets the clear output. The system designed in this paper has 2 inputs e and de, 1 output μ, and each input has 3 fuzzy subsets. There are 9 fuzzy rules, and each rule has 1 output. Finally, the output is synthesized into one output μ by output function.

Fuzzy rules of the TS fuzzy inference machine are shown in Table 1. Because of its own characteristics, the first order TS fuzzy inference machine system do not need to be deblurring, and the

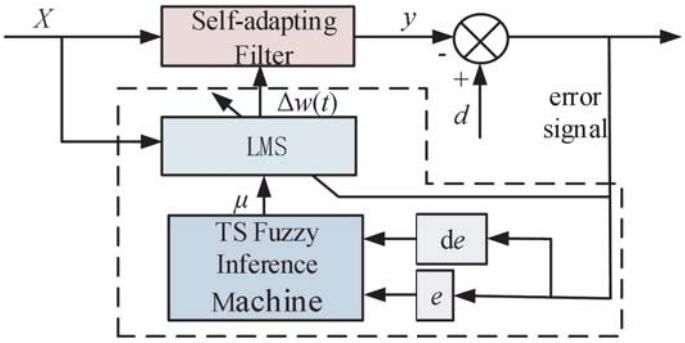

Figure 9. Fuzzy adaptive filter.

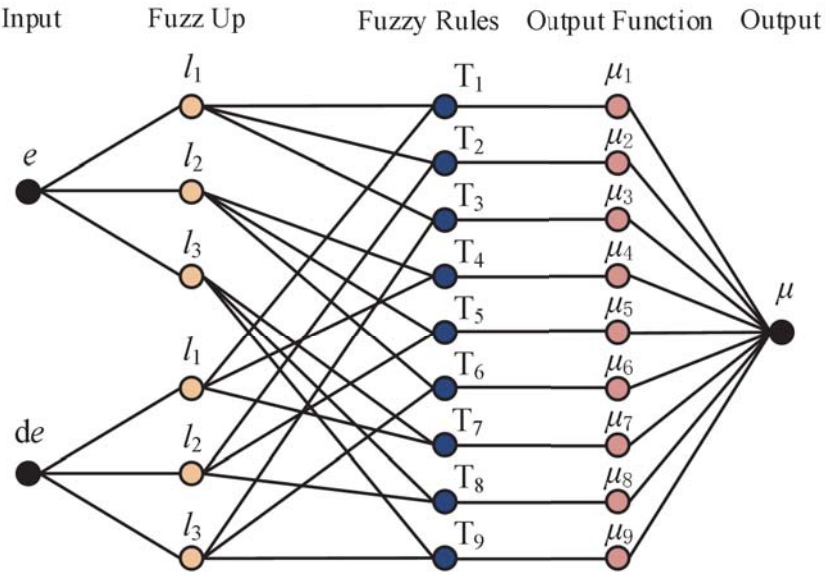

Figure 10. Fuzzy control structure.

Table 1. Fuzzy control rules.

Error e	Error variation de	Step size μ
S	N	S
S	Z	S
S	P	M
M	N	S
M	Z	M
M	P	L
L	Z	L
L	P	L

final output is obtained by weighted average of each fuzzy rule output according to its corresponding weights.

4. SIMULATION AND EXPERIMENT

4.1. Experimental Platform

The experiment was carried out on the experimental platform shown in Fig. 11. The experimental device mainly includes eddy current displacement sensor, displacement signal interface circuit, DSP controller minimum system, DC power supply, radial power drive board, AC power supply, personal computer (PC), DSP simulator, etc.

Basic parameters of the six-pole radial HMB: the air gap length of the HMB prototype is 0.5 mm; the saturation magnetic induction intensity is 0.8 T; the radial magnetic pole area is 260 mm^2; the maximum installed turn number of the radial coil is 160; the magnetomotive force of the permanent magnet is 320 At; the radial width of the magnetic pole is 16 mm; the axial width of the permanent magnet is 3 mm; the length of the magnetic bearing is 25 mm; and the maximum radial bearing capacity can be 200 N.

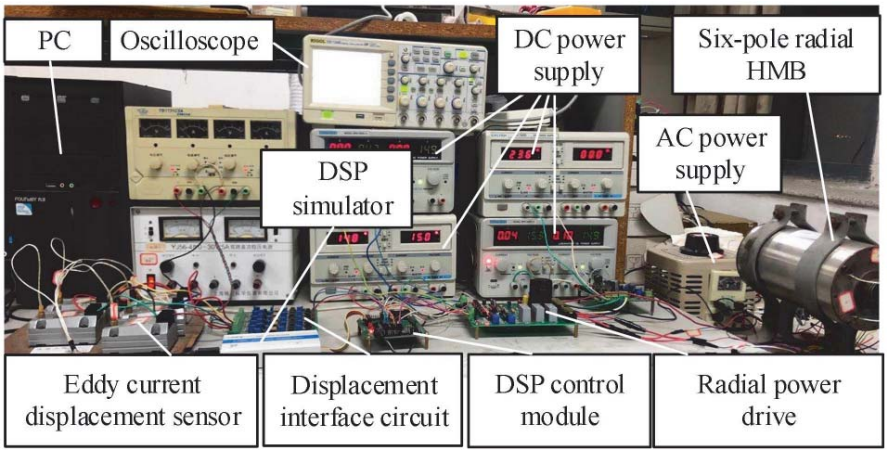

Figure 11. Experimental platform.

4.2. Simulation Analysis

The vibration signal is simulated by sine wave in the simulation software Matlab; the amplitude is 0.5 V; the setting frequency f is 250 Hz, as shown in Fig. 12. The frequency can be dynamically adjusted according to the experimental needs. Since the eddy current sensor is used in the experiment, the output voltage range is $-18\,\mathrm{V} \sim -2\,\mathrm{V}$. When the rotor is stably suspended, the output voltage of the sensor is about -10 V, so the voltage at the balance position of the simulated rotor is -10 V. Algorithm step size of the adaptive filter μ takes the fixed values of 0.06 and 0.6, respectively, compared with the fuzzy adaptive filter which uses the fuzzy step size. The simulation diagrams of the unbalance vibration compensation effect are shown in Fig. 12, Fig. 13, Fig. 14, respectively.

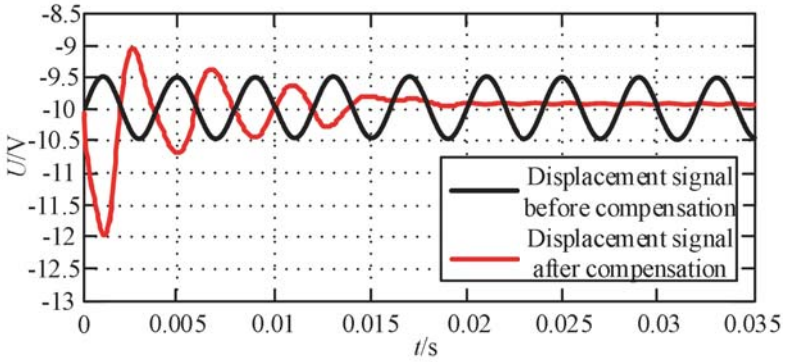

Figure 12. The displacement signal when μ is 0.06.

As Fig. 12 shows, when the algorithm step size of the adaptive filter μ is 0.06, the magnetic bearing rotor realizes the compensation of unbalance vibration after 0.017 s. At this time, the amplitude of displacement signal after compensation is 0.05 V, and it differs from the target equilibrium position by 0.1 V.

As Fig. 13 shows, the algorithm step size of the adaptive filter μ is 0.6, and the time for the magnetic bearing rotor system to realize the unbalance vibration compensation is 0.007 s. Compared with the algorithm where μ is 0.06, the tracking time of the adaptive filter is greatly reduced. The amplitude of displacement signal after compensation is 0.18 V; the amplitude is relatively large; and the difference from the simulated rotor equilibrium position is close to 1 V.

When the adaptive filter adopts the fuzzy step size LMS algorithm, as shown in Fig. 14, the magnetic

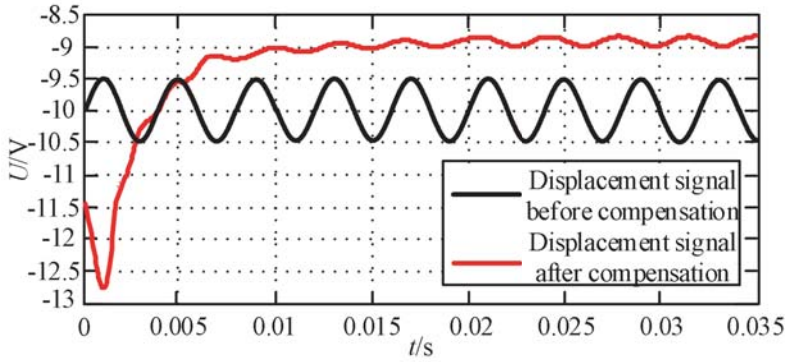

Figure 13. The displacement signal when μ is 0.6.

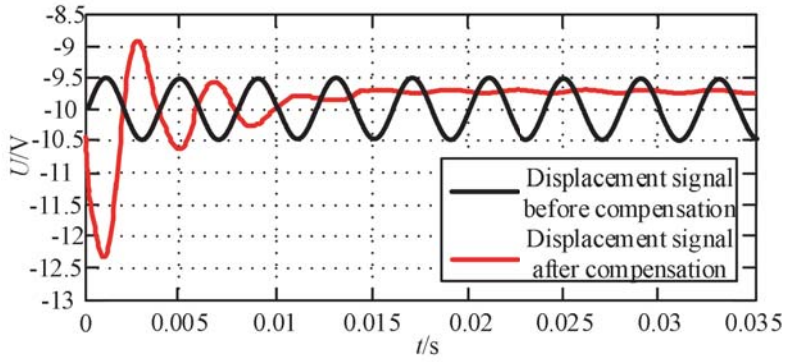

Figure 14. The displacement signal after vibration compensation when using fuzzy step size.

bearing rotor system realizes the compensation of unbalance vibration after 0.01 s. The amplitude of the compensated displacement signal is only 0.09 V, and the difference from the equilibrium position is only 0.3 V.

It can be seen that when the step size of adaptive filter algorithm takes a large fixed value, its convergence speed is fast. The tracking ability is strong, and the vibration compensation can be realized quickly. However, the amplitude of the displacement signal after compensation is large, and the difference from the rotor balance position is large. When the step size of adaptive filter algorithm takes a small fixed value, the amplitude of the displacement signal after compensation is small, and the displacement signal is close to the rotor equilibrium position, but the tracking speed is too slow to meet the requirement of real-time compensation when the rotor changes speed. It can be seen from Fig. 14 that when the fuzzy step size LMS algorithm is used, the magnetic bearing can realize the unbalance vibration compensation smoothly. The amplitude of the displacement signal after compensation is small, and the rotor is close to the equilibrium position. Because its step size can be adjusted according to the feedback error signal, when the rotor vibration is large at the beginning, the larger step size is used to accelerate the tracking speed, which makes up for the problem that the tracking speed is too slow to realize the vibration compensation in real time when the smaller fixed step size is taken.

4.3. Experiment Research

Considering that the speed changes dramatically when the magnetic bearings are floating and stopping, the algorithm with strong tracking ability is needed. When μ is small, it is obvious that the tracking time is too long to meet the real-time compensation requirement. Therefore, we choose the LMS algorithm with large fixed step size μ which is 0.6 and the fuzzy step size LMS algorithm to experiment and compare the performance of their vibration compensation.

When the compensation measure for unbalance vibration has not been implemented, the motion

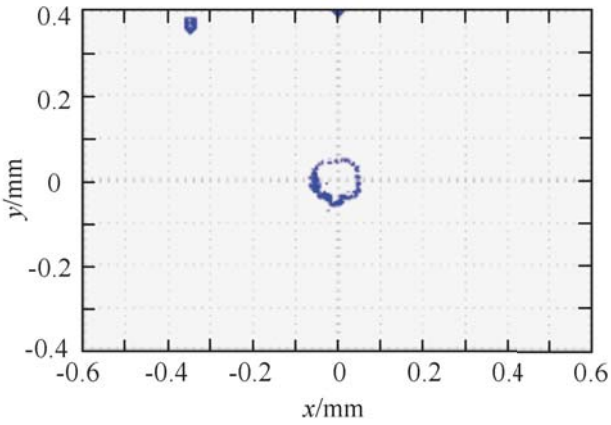

Figure 15. The rotor trajectory without vibration compensation.

trajectory of the magnetic bearing rotor is shown in Fig. 15. It can be seen from the diagram that the rotor's motion trajectory is annular, and the track diameter reaches 0.12 mm. The rotor is greatly affected by centrifugal force, which makes the rotor unbalance vibration occur during operation and seriously affects the operation accuracy of the magnetic bearing rotor system.

Figure 16 shows the motion trajectory of the rotor after the vibration compensation control is applied. At this time, the filtering algorithm of the filter adopts a fixed step size LMS algorithm, and the step size is set as 0.6. It can be seen from the diagram that the motion trajectory of the rotor after compensation is obviously gathered to the center, and the trajectory diameter is reduced to 0.06 mm, which means that the method achieves the expected compensation effect. However, the steady-state error is large, that is, the amplitude of the rotor after compensation is relatively large, and it differs significantly from the target equilibrium position of the rotor.

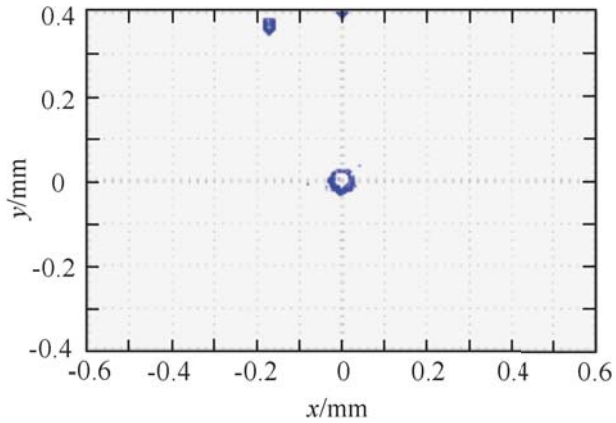

Figure 16. The rotor trajectory when μ is 0.6.

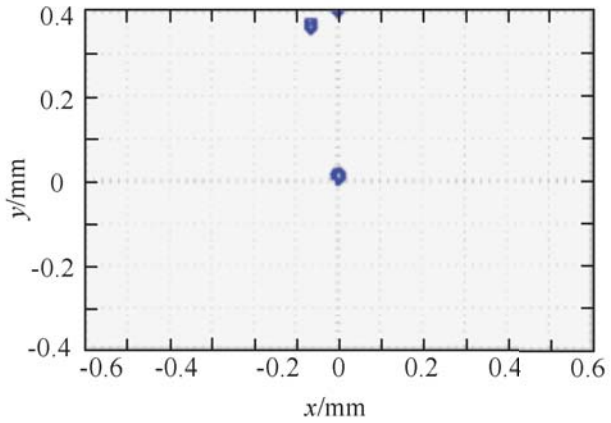

Figure 17. The rotor trajectory when using fuzzy μ.

As Fig. 17 shows, fuzzy step size LMS algorithm is used as filter adaptive algorithm to implement unbalance vibration compensation. The algorithm step size is adjusted adaptively by fuzzy inference system according to feedback error signal. It can be seen from the diagram that the rotor's amplitude is obviously reduced after compensation, and the rotor motion trajectory diameter is reduced to 0.03 mm. The compensation effect is obvious. In addition, the steady-state error of the compensated rotor is smaller, and the rotor is closer to the target equilibrium position.

Figures 18 and 19 are the displacement response curves of the rotor after vibration compensation

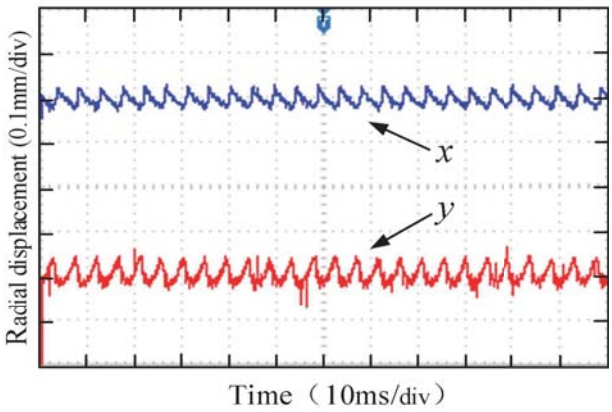

Figure 18. The displacement when μ is 0.6.

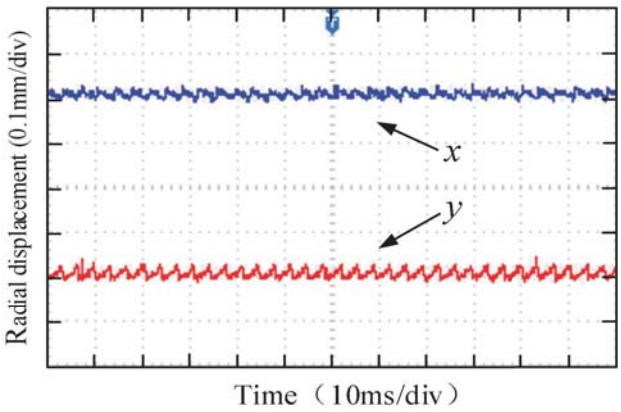

Figure 19. The displacement when using fuzzy μ.

when the algorithm step size is 0.6 and the fuzzy step size, respectively. It can be seen from the diagram that when the control strategy of fuzzy step size algorithm is adopted, its compensation effect is more obvious.

Experimental results show that when the fuzzy LMS algorithm is selected as the filtering algorithm, the amplitude of the compensated rotor is smaller, which is closer to the target equilibrium position, and the compensation effect is more obvious. Because the step size can be adjusted according to the external error signal, when the rotor vibration is large, a larger step size is used to speed up the tracking speed, which can satisfy the real-time vibration compensation at the same time. As the magnetic bearing is applied in the field of high precision, the fuzzy LMS algorithm described in this paper can show its superiority.

5. CONCLUSIONS

An unbalance vibration compensation control method for six-pole radial HMB rotor system based on a fuzzy adaptive filter is presented. Fuzzy step size LMS algorithm is used as adaptive filtering algorithm, and fuzzy control system is used to adjust the step size of the algorithm. When the initial stage of the system operation or the speed change is large, a larger step size is used to speed up the filter tracking speed to improve the real-time performance of the vibration compensation. When the system tends to be stable, and the rotor vibration is suppressed, a smaller step size is used to obtain a smaller steady-state misalignment, which improves the compensation accuracy and makes the rotor closer to the target equilibrium position. Comparing the proposed fuzzy adaptive filter with the filter with the fixed step size LMS algorithm in vibration compensation effect, it can be found that the proposed fuzzy adaptive filter has obvious advantages. The simulated and experimental results show that the proposed method of rotor unbalance vibration compensation control has the advantages of adopting larger algorithm step size and smaller algorithm step size. It meets the requirements of real-time compensation and small steady-state error at the same time, and greatly improves the compensation effect, which is suitable for high precision applications.

ACKNOWLEDGMENT

This project is supported by the National Natural Science Foundation of China (61973144, 51675244) and Priority Academic Program Development of Jiangsu Higher Education Institution (PAPD-2018-87).

REFERENCES

1. Ju, J.-T. and H.-Q. Zhu, "Radial force-current characteristics analysis of three-pole radial-axial hybrid magnetic bearings and their structure improvement," *IET Electr. Power Appl.*, Vol. 11, No. 9, 1548–1557, 2017.
2. Le, Y., J.-J. Sun, and B.-C. Han, "Modeling and design of 3-DOF magnetic bearing for high-speed motor including eddy-current effects and leakage effects," *IEEE Trans. Ind. Electron.*, Vol. 63, No. 6, 3656–3665, 2016.
3. Zhu, D.-H., X. Cheng, and H.-Q. Zhu, "Structure and performance analysis for AC-DC three degrees of freedom active magnetic bearings," *Proc. 2009 IEEE 6th International Power Electronics and Motion Control Conference*, 2005–2009, 2009.
4. Zhang, W.-Y., H.-Q. Zhu, Z.-B. Yang, et al., "Nonlinear model analysis and "switching model" of AC-DC three-degree-of-freedom hybrid magnetic bearing," *IEEE/ASME Trans. Mechatronics*, Vol. 21, No. 2, 1102–1115, 2016.
5. Zhang, W.-Y. and H.-Q. Zhu, "Control system design for a five-degree-of-freedom electrospindle supported with AC hybrid magnetic bearings," *IEEE/ASME Trans. Mechatronics*, Vol. 20, No. 5, 2525–2537, 2015.
6. Zhang, W.-Y. and H.-Q. Zhu, "Improved model and experiment for AC-DC three-degree-of-freedom hybrid magnetic bearing," *IEEE Trans. Magnetics*, Vol. 49, No. 11, 5554–5565, 2013.
7. Wu, H.-T., J. Zhou, and L. Ji, "Unbalance compensation of magnetically suspended rotor based on single phase coordinate transformation," *Journal of Zhejiang University (Engineering Science)*, Vol. 54, No. 5, 963–971, 2020.
8. Inoue, T., J. Liu, Y. Yoshimura, et al., "Vibration control and unbalance estimation of a nonlinear rotor system using disturbance observer," *J. Vib. Acoust.*, Vol. 131, No. 3, 031010–031018, 2009.
9. Peng, C., M.-T. Zhu, K. Wang, et al., "A two-stage synchronous vibration control for magnetically suspended rotor system in the full speed range," *IEEE Trans. Ind. Electron.*, Vol. 67, No. 1, 480–489, 2020.
10. Mao, C. and C.-S. Zhu, "A Real-time variable step size iterative unbalance compensation for active magnetic bearing-rigid rotor systems," *Proceedings of the CSEE*, Vol. 38, No. 13, 3960–3968, 2018.
11. Peng, C., J.-J. Sun, C.-X. Miao, and J.-C. Fang, "A novel cross-feedback notch filter for synchronous vibration suppression of an MSFW with significant gyroscopic effects," *IEEE Trans. Ind. Electron.*, Vol. 64, No. 9, 7181–7190, 2017.
12. Yoon, S.-Y., L. Di, and Z.-L. Lin, "Unbalance compensation for AMB systems with input delay: An output regulation approach," *Control Eng. Practice*, Vol. 46, 166–175, 2016.
13. Mao, C. and C.-S. Zhu, "Unbalance compensation for active magnetic bearing rotor system using a variable step size real-time iterative seeking algorithm," *IEEE Trans. Ind. Electron.*, Vol. 65, No. 5, 4177–4186, 2018.
14. Cui, P.-L., S. Li, Q.-R. Wang, et al., "Harmonic current suppression of an AMB rotor system at variable rotation speed based on multiple phase-shift notch filters," *IEEE Trans. Ind. Electron.*, Vol. 63, No. 11, 6962–6969, 2016.
15. Liu, C. and G. Liu, "Autobalancing control for MSCMG based on sliding-mode observer and adaptive compensation," *IEEE Trans. Ind. Electron.*, Vol. 63, No. 7, 4346–4356, 2016.
16. Wang, Z.-B., C. Mao, and C.-S. Zhu, "Current compensation control of multiple frequency vibrations of the rotor in active magnetic bearing high speed motors," *Proceedings of the CSEE*, Vol. 38, No. 1, 275–284, 2018.
17. Cui, P. and J. Cui, "Harmonic current suppression of active-passive magnetically suspended control moment gyro based on variable-step-size FBLMS," *J. Vib. Control*, Vol. 23, No. 8, 1221–1230, 2015.